Ab Initio Studies of Disilazanes: Structures and Vibrational Properties of Hexachloro-, Hexamethyl-, and Tetrachlorodisilazane

Holger Fleischer

Institut für Anorganische Chemie und Analytische Chemie, Johannes Gutenberg Universität, Johann Joachim Becher Weg 24, D-55099 Mainz, Germany

Donald C. McKean*

Department of Chemistry, University of Edinburgh, West Mains Road, Edinburgh EH9 3JJ, U.K.

Received: July 21, 1998; In Final Form: November 18, 1998

The structures of hexachlorodisilazane, $NH(SiCl_3)_2$, and hexamethyldisilazane, $NH(SiMe_3)_2$, have been calculated at HF/6-31G* and MP2/6-31G* levels. Both contain planar $HNSi_2$ skeletons and show the expected staggering of the substituents as seen along the Si···Si direction, as previously found in the electron diffraction structure of the hexamethyl compound. Unlike the latter, however, the ab initio structures both belong to the C_2 point group. Force fields for these two molecules and for tetrachlorodisilazane, $NH(SiHCl_2)_2$, were calculated at the HF level and scaled to produce vibration frequencies for comparison with previously obtained spectra. For $NH(SiCl_3)_2$, all but five of the fundamentals are satisfactorily assigned. Seven scale factors could be refined, other factors being transferred from model compounds. For the hexamethyl compound, the interpretation was less detailed. In all three molecules the out-of-plane NH bending motion is found to be associated with fundamentals around or below 400 cm^{-1}, far lower than previous assignments. The force constant for this motion is greatly reduced as chlorine substituents are replaced by methyl groups, which shows the sensitivity of the stability of the planar system to the inductive effect of substituents. For tetrachlorodisilazane, $NH(SiHCl_2)_2$, earlier spectra were reanalyzed and evidence was found for the presence of two conformers, as suggested by previous ab initio investigations. The vibrational properties of the SiH bonds were explored by extending the ab initio calculations to a series of nonequilibrium structures, with the object of mapping variations in the SiH bond with change in torsional angle. This bond is strongest in the skeletal plane and weakest at right angles to the latter, which is in accordance with an n(N)−σ*(Si−H) orbital interaction. However the orientation of the other silyl group also influences SiH bond strength. Long-range interactions are found between the stretching motions of both SiH and SiCl bonds. The former appear to arise from dipole−dipole interactions between the SiH bonds, but the source of the latter remains obscure. The form of the observed νSiH spectrum suggests that signal averaging conceals the splittings expected from both interactions and bond strength variation. Electrical properties of the SiH and SiCl bonds are examined.

Introduction

Disilazanes of the type $NR(SiXYZ)_2$ have been of interest to the theoretical chemist since the first determinations of structure in $N(SiH_3)_3$, $NH(SiH_3)_2$, and $NMe(SiH_3)_2$ by the gas-phase electron diffraction method indicated that the $RNSi_2$ skeleton was planar and accompanied by a wide SiNSi angle.[1−5] The same has found to be true in all derivatives subsequently studied.[6−12]

Particular attention has been given in these studies to the mutual orientation of the substituents on the two silicon atoms, which in the case of asymmetrically substituted $SiXY_2$ groups can lead to a variety of conformers. The structural principle found to govern conformation is the tendency for bulky substituents to be staggered when viewed along the Si···Si direction.[12] In the special case of $NR(SiHMeCl)_2$ compounds, diastereoisomers will in general be present and have been detected by the combined use of spectroscopic, ab initio, and electron diffraction methods.[12,13]

In systems involving $SiHMe_2$ and SiH_2Me groups, structural evidence obtained by the electron diffraction method has been supported by infrared studies in the SiH stretching region near 2200 cm^{-1}.[14]

A curious feature of these systems is the appearance of two νSiH bands in all the spectra of $NMe(SiHXY)_2$ compounds but only a single band for the NH analogues. The splitting in the former series has been analyzed in terms of a variation with torsional angle in the individual SiH bond stretching frequencies ("ν^{is}SiH" values), together with a long-range interaction beween the stretchings of the two SiH bonds.[13] While these effects are also present in the NH compounds, signal averaging appears to be the source of the single broad band seen.

Of the three compounds studied in the present work, $NH(SiCl_3)_2$ has been the subject of an infrared and Raman investigation followed by an empirical force field for those vibrations associated with the A_1 and B_1 species of an assumed C_{2v} structure,[15] no electron diffraction or other structural study having yet been made. In this structure, the chlorine atoms eclipse each other when viewed along the Si···Si direction, which now seems unlikely in light of the electron diffraction evidence noted above.

For the second molecule, $NH(SiMe_3)_2$, an electron diffraction structural study shows planarity of the $HNSi_2$ system and an almost staggered arrangement of the $SiMe_3$ groups viewed along the Si···Si direction, the overall symmetry being C_1.[6] A number of spectral studies are available.[16−20]

10.1021/jp983104t CCC: $18.00
Published on Web 01/22/1999

A feature of the assignments in the latter is a gross uncertainty as to the location of the out-of-plane NH bend, $\delta_{\perp}$NH. The lowest estimate for the latter is 774 cm^{-1}.[19]

The stiffness of this motion is a direct measure of the forces imposing planarity in a system which, were two or three methyl groups rather than silyl ones to be involved, would be pyramidal. There is therefore a general interest in identifying the positions of this mode in the spectra, or at least its associated force constant, for molecules of the type $NH(SiXYZ)_2$ and relating these to the effect of substituents.

The third molecule, $NH(SiHCl_2)_2$, was first studied by vibrational spectroscopy, and the spectra were interpreted as favoring a C_s structure.[21] In a recent joint ab initio and electron diffraction investigation,[11] MP2/6-31G* calculations indicated the presence of two minima in the potential surface, both having SiH bonds in the skeletal plane with point groups and pairs of HNSiH dihedral angles respectively C_{2v} (180°,180°) and C_s (0°,180°), their abundancies being 43% and 57%. However the barrier between the two conformations was very low, as reflected in a low torsional frequency of 5 cm^{-1}, which indicates very easy rotation about the SiN bond. The electron diffraction analysis carried out on the basis of these two ab initio structures yielded a slightly higher *R* factor than that based on either of two single structures, the first of these, with HNSiH angles of 146°,155°, being nearly staggered along the Si···Si axis and the second, a 131°,80° structure, being nearly eclipsed in this sense. However, no firm conclusion could be drawn from the electron diffraction evidence about the presence or absence of more than one conformer.

The ab initio result that the 180°,180° structure has the lowest energy is of interest in that this structure is completely eclipsed, by contrast to the preference for staggered structures established earlier for other compounds.[12] A likely explanation for this is a greater importance of n(N)−σ*(Si−Cl) interactions in this molecule.

While complete vibrational analyses of molecules of this kind remain a distant prospect, the availability of ab initio force fields supplemented by judicious scaling should provide a much improved understanding of existing spectra, particularly in relation to the structure(s) which may be present. The scale factors needed for such an exercise will in many cases need to be transferred from model compounds of similar structure for which good assignments can be made. Such compounds are SiH_3SiHCl_2,[22] $NMe(SiH_3)_2$, and $SiHMe_3$.[23] $NMe(SiHCl_2)_2$ has been a recent example of such a study.[24]

The present work forms part of an ongoing study of silazanes which includes $NH(SiH_3)_2$, $NMe(SiH_3)_2$, and $N(SiH_3)_3$.

Theoretical Section

The ab initio calculations were carried out using the Gaussian 94 program.[25] For $NH(SiCl_3)_2$, and $NH(SiMe_3)_2$, optimized geometries and analytical Cartesian force constants were obtained using Hartree−Fock theory and the 6-31G* basis set.[26] Optimization was also carried out at the MP2/6-31G* level. In both cases, the "tight" option for convergence on the final geometry was employed in order to ensure that the fourth decimal place in the bond lengths was significant. However, calculations without this condition indicated that this precaution was unnecessary. Earlier data on $NH(SiHCl_2)_2$[11] obtained at these levels were supplemented by further HF/6-31G* calculations undertaken for us by Dr. M. Bühl at the University of Zürich. In all cases, the output from Gaussian 94 of Cartesian force constants was introduced into the program ASYM40, an update of ASYM20,[27] for transformation into internal coordinates followed by scaling according to the method of Pulay et al.[28] The latter scales off-diagonal symmetry force constants by the geometric mean of the corresponding diagonal ones.

A feature of the additional calculations performed for $NH(SiHCl_2)_2$ was the optimization of structures in which the orientations of the two silyl groups were fixed at chosen torsional angles. This was to permit an exploration of the conformational dependence of the SiH bond distance and force constant. Such structures not being equilibrium ones, in general they give rise to at least one imaginary vibration frequency. In principle, the presence of a nonzero force in an otherwise fully optimized structure can render the subsequent calculation of frequency meaningless. However, we consider that the nature of the constraint which we apply can only perturb the lowest part of the vibrational spectrum, where the torsional modes are located, and leave the upper part, where the stretchings of the SiH bonds are to be found, undisturbed and meaningful. The consistency of the results obtained there supports our belief.

However, for all exercises which involved scaling of the ab initio force field, as was needed for analysis of the complete spectrum, only equilibrium structures could be treated, since ASYM40 cannot handle imaginary frequencies. Thus for $NH(SiHCl_2)_2$, we were obliged to treat the C_2 (171.5°,171.5°) structure predicted at the HF/6-31G* level, rather than the almost identical C_{2v} (180°,180°) one, which is an equilibrium structure only at the MP2/6-31G* level, not in the HF/6-31G* calculation.[11]

In addition to calculations of frequency, we include in this work electrical properties associated with the bonds or atoms concerned.

The Gaussian 94 program outputs not only the Mulliken charges for all the atoms but also the dipole derivatives of each atom with respect to their Cartesian displacements in a space-fixed frame, $\partial p_\alpha/\partial\alpha$ ($\alpha = x, y, z$), the elements of the so-called atomic polar tensor $\mathbf{P}_a$.[29] Associated with the latter are various invariants, of which the King effective charge ξ_a,[30] defined for each atom *a* by

$$\xi_a^{\,2} = (\mathbf{P}_a)'\cdot(\mathbf{P}_a)$$

is the most quoted (alternatively quoted as $\chi = 3^{-1/2}\xi$). This quantity reflects all the intensities associated with both vibrations and rotations of the molecule. If, for a terminal atom, the axes with reference to which the atomic polar tensor is defined are rotated so that one axis lies along the bond concerned, then the corresponding column elements of the tensor give the components of the dipole derivative with respect to the stretching of that bond, $\partial\boldsymbol{\mu}/\partial r$, from which the magnitude and direction of the vector $\partial\boldsymbol{\mu}/\partial r$ can be obtained.

For SiH bonds, where the degree of local mode behavior is very high, this will be the only electrical quantity of importance in determining the intensities of the SiH stretching vibrations. In principle, the chemical interest in such properties is as great as that in force constants and the only reason for the comparatively little attention paid to them lies in the difficulty of obtaining such data experimentally. The availability of such information from ab initio sources therefore provides a welcome opportunity not to be missed.

Results and Discussion

$NH(SiCl_3)_2$. The structure of this molecule as determined ab initio belongs to the C_2 point group. When viewed along the Si···Si direction, as in Figure 1, the staggering of the chlorines

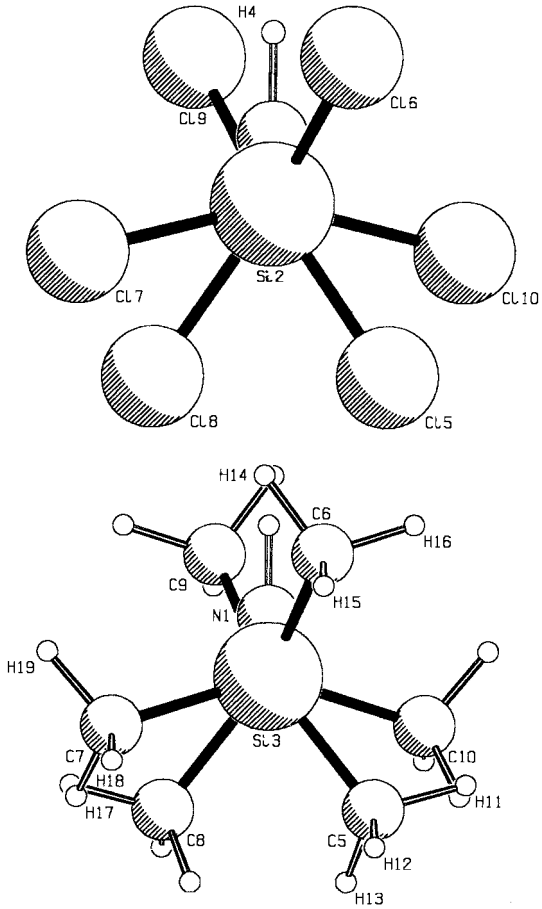

Figure 1. HF/6-31G* C_2 structures of $NH(SiCl_3)_2$ (top) and $NH(SiMe_3)_2$ (bottom), viewed along the Si···Si direction.

TABLE 1: Ab Initio Geometries (6-31G* Basis) and Internal Coordinates for $NH(SiCl_3)_2$, C_2 Symmetry

bond length/angle[a]	HF	MP2	internal coordinates
*r*N(1)Si(2), *r*N(1)Si(3)	1.7137	1.7243	r_2, r_3
rN(1)H(4)	1.0054	1.0208	r_4
*r*Si(2)Cl(5), *r*Si(3)Cl(8)	2.0316	2.0294	r_5, r_8
*r*Si(2)Cl(6), *r*Si(3)Cl(9)	2.0382	2.0355	r_6, r_9
*r*Si(2)Cl(7), *r*Si(3)Cl(10)	2.0362	2.0341	r_7, r_{10}
∠Si(2)N(1)Si(3)	134.6	131.3	$\gamma_{2,3}$
∠H(4)N(1)Si(2), ∠H(4)N(1)Si(3)	112.7	114.4	$\gamma_{2,4}$, $\gamma_{3,4}$
∠N(1)Si(2)Cl(5), ∠N(1)Si(3)Cl(8)	110.5	109.7	$\beta_{2,5}$, $\beta_{3,8}$
∠N(1)Si(2)Cl(6), ∠N(1)Si(3)Cl(9)	107.0	107.0	$\beta_{2,6}$, $\beta_{3,9}$
∠N(1)Si(2)Cl(7), ∠N(1)Si(3)Cl(10)	112.3	112.5	$\beta_{2,7}$, $\beta_{3,10}$
∠Cl(5)Si(2)Cl(6), ∠Cl(8)Si(3)Cl(9)	110.3	110.8	$\alpha_{5,6}$, $\alpha_{8,9}$
∠Cl(5)Si(2)Cl(7), ∠Cl(8)Si(3)Cl(10)	108.4	108.4	$\alpha_{5,7}$, $\alpha_{8,10}$
∠Cl(6)Si(2)Cl(7), ∠Cl(9)Si(3)Cl(10)	108.2	108.4	$\alpha_{6,7}$, $\alpha_{9,10}$
⟨Cl(5)Si(2)N(1)Si(3), ⟨Cl(8)Si(3)N(1)Si(2)	36.8	37.0	$\tau_{3,5}$, $\tau_{2,8}$
⟨Cl(6)Si(2)N(1)Si(3), ⟨Cl(9)Si(3)N(1)Si(2)	156.9	157.3	$\tau_{3,6}$, $\tau_{2,9}$
⟨Cl(7)Si(2)N(1)Si(3), ⟨Cl(10)Si(3)N(1)Si(2)	−84.4	−83.8	$\tau_{3,7}$, $\tau_{2,10}$
⟨N(1)Si(2)Si(3)H(4)	0.0	0.0	$w_{1,2,3,4}$
⟨Cl(6)Si(2)N(1)H(4), ⟨Cl(9)Si(3)N(1)H(4)	−23.1	−22.7	
⟨Cl(6)Si(2)Si(3)Cl(9)	−56.4	−56.9	

[a] ⟨ denotes a dihedral angle. Bond lengths in angstroms; angles in degrees. Atom numbering as in Figure 1.

is clearly seen. The geometrical parameters determined are very similar at the HF and MP2 levels, as shown in Table 1, the largest difference being one of 3.3° in the SiNSi angle.

Table 2 lists the vibrational quantities calculated for the d_0 and d_1 species, together with the scaled frequencies and potential energy distributions. Tables 3 and 4 give the symmetry coordinates, scale factors, and symmetry force constants respectively.

With an initial transfer of scale constants from other molecules, a pleasing number of assignments of the observed bands could be made, ten out of twelve in the A symmetry species and nine out of twelve in the B species. The most interesting of these from a structural point of view is the $\delta_\perp$NH bending mode, which is identified at 390 cm^{-1} for the d_0 species, shifting to a coupled mode at 367 cm^{-1} for the d_1 one.

In several cases, pairs of frequencies belonging to the A and B symmetry species are predicted close together with rather different infrared and Raman intensities. On the basis of such intensities, we consider that the frequency observed at 472 cm^{-1} in the infrared spectrum has an origin different from that at 476 cm^{-1} in the Raman spectrum, as indicated in Table 2.

The final refinement of scale factors was limited to seven independent parameters, as listed in Table 3. While the symmetric and asymmetric NSi_2 stretches required differing values, there was insufficient evidence for similar differences to be discerned in the SiCl stretches, the problem being overlap between intense and closely spaced bands.

A small improvement in the fit resulted from allowing the $\delta_{as}SiCl_3$ and δ_sSiCl_3 factors to refine. When the $\rho SiCl_3$ factors were similarly allowed to float, the scale factor for the $\delta_\perp$NH motion drifted rather lower than seemed probable, with very little improvement in the fit. The skeletal bends other than the $\delta SiCl_3$ ones were therefore constrained to transferred values. Even so, the factors for both the $\delta_{||}$NH and $\delta_\perp$NH bending motions are lower than is usual, particularly the latter.

In Table 5A, we compare some valence force constants in our work with those from the previous empirical force field.[15] The agreement is good between the two sets of values except for the NSi−NSi stretch−stretch interaction, which is rather larger in the ab initio calculation. In Table 5B, we list interactions between the stretches of the SiCl bonds, which are significant even between bonds on different silicons, indicating a long-range interaction of some kind. A rough correlation with the ClSiSiCl torsional angle is evident. In Table 5C, we show values of $\partial\boldsymbol{\mu}/\partial r$ for the SiCl bond which also vary with orientation and partly at least reflect changes in the Mulliken atomic charge.

$NH(SiMe_3)_2$. The HF/6-31G* structure determined for $NH(SiMe_3)_2$ is shown in Figure 1, the parameters for this and the MP2 structure being listed in Table 6. As for $NH(SiCl_3)_2$, the point group is found to be C_2, with a staggered configuration rather close to that for the $SiCl_3$ compound. There is a similar difference in the NSi_2 angle between the HF and MP2 calculations compared to that found for $NH(SiCl_3)_2$, but the skeletal torsional angles CSiNH are essentially identical at the two levels and doubt must therefore be cast on the asymmetry present here in the electron diffraction structure.[6] There is also a marked disagreement with the ED structure over the HCSiN torsional angles, the methyl groups in the ab initio structure being almost exactly staggered, which is not the case in the ED structure. This we attribute to the low scattering contributions of the H atoms.

We note that the ED structure[9] of $NMe(SiMe_3)_2$ also has a C_2 skeleton, but since the CSiNH dihedral angle there is −38.4°, it is rather more staggered when viewed along the Si···Si direction than we find here for the NH compound.

In analyzing the vibrational spectra, there is little point in attempting to distinguish each of the methyl group internal modes, other than the rocking motions expected in the region below 900 cm^{-1}. Table 7 therefore lists data for the remaining 21 modes in each of the A and B symmetry species.

TABLE 2: Ab Initio Vibrational Data and Observed Frequencies for Hexachlorodisilazanes

A. $NH(SiCl_3)_2$

mode	ν_{unsc}[a]	A[b]	R[c]	dp[d]	ν_{sc}[e]	ν_{obs}[f]	PED[g]	motion
A								
ν_1	3746	89	48	0.28	3356	3356[h]	$100S_1$	νNH
ν_2	802	234	1	0.51	767	767[h]	$72S_2$, $10S_3$	$\nu_s NSi_2$
ν_3	673	271	2	0.21	632	626[h]	$30S_3$, $58S_4$	$\nu_{as}SiCl_3$
ν_4	636	6	4	0.74	597	595[i]	$20S_3$, $21S_4$, $68S_5$	$\nu_{as}SiCl_3$
ν_5	504	5	14	0.02	470	476[i]	$40S_3$, $19S_5$, $14S_6$	$\nu_s SiCl_3$
ν_6	358	0	7	0.05	336	335[i]	$22S_4$, $11S_6$, $21S_7$	cpld[j]
ν_7	230	0	4	0.75	216	213[i]	$54S_8$, $14S_{11}$	$\delta_{as}SiCl_3$
ν_8	204	10	2	0.75	194	194[h]	$19S_7$, $75S_9$	$\delta_{as}SiCl_3$
ν_9	150	0.4	2	0.69	142	146[i]	$46S_7$, $23S_9$, $12S_{10}$	$\delta_s SiCl_3$
ν_{10}	133	0	3	0.74	124	130[k]	$44S_8$, $35S_{10}$, $53S_{11}$	$\rho SiCl_3$
ν_{11}	73	1	0.3	0.74	67		$61S_6$, $22S_{10}$, $13S_{11}$	δNSi_2
ν_{12}	24	0	0	0.56	22		$106S_{12}$	$\tau SiCl_3$
B								
ν_{13}	1390	332	0.1		1223	1215[h]	$23S_{13}$, $85S_{17}$	$\delta_{\parallel}$NH
ν_{14}	1024	450	0.1		966	975[h]	$82S_{13}$, $14S_{17}$	$\nu_{as}NSi_2$
ν_{15}	671	585	1		623	617[h]	$32S_{14}$, $58S_{16}$	$\nu_{as}SiCl_3$
ν_{16}	637	63	4		597	600[h]	$38S_{14}$, $67S_{15}$	$\nu_{as}SiCl_3$
ν_{17}	499	103	0.2		468	472[h]	$29S_{14}$, $30S_{15}$, $31S_{16}$, $10S_{19}$	$\nu_s SiCl_3$
ν_{18}	448	36	1		388	390[h]	$57S_{18}$, $13S_{22}$, $28S_{23}$	$\delta_{\perp}$NH
ν_{19}	304	0.2	0.4		267		$38S_{18}$, $20S_{22}$, $19S_{23}$	$\rho SiCl_3$
ν_{20}	268	41	1		254	250[h]	$85S_{19}$	$\delta_s SiCl_3$
ν_{21}	221	8	4		209	208[h]	$66S_{21}$	$\delta_{as}SiCl_3$
ν_{22}	182	5	0.5		172	174[h]	$99S_{20}$, $11S_{23}$	$\delta_{as}SiCl_3$
ν_{23}	129	0.7	2		119		$19S_{18}$, $36S_{21}$, $45S_{22}$, $49S_{23}$	$\rho SiCl_3$
ν_{24}	25	1	0.1		23		$35S_{22}$, $17S_{23}$, $151S_{24}$	$\tau SiCl_3$

B. $ND(SiCl_3)_2$

mode	ν_{unsc}[a]	A[b]	R[c]	dp[d]	ν_{sc}[e]	ν_{obs}[f,h]	PED[g]	motion
A								
ν_1	2738	68	23	0.31	2454	2484	$100S_1$	νND
ν_2	793	230	1	0.56	757	757	$71S_2$, $11S_3$	$\nu_s NSi_2$
ν_3	673	271	2	0.21	632	623	$30S_3$, $58S_4$	$\nu_{as}SiCl_3$
ν_4	636	6	4	0.74	597		$20S_3$, $21S_4$, $68S_5$	$\nu_{as}SiCl_3$
ν_5	497	3	14	0.02	464		$39S_3$, $19S_5$, $13S_6$	$\nu_s SiCl_3$
ν_6	357	0	7	0.05	335		$21S_4$, $12S_6$, $21S_7$	cpld[j]
ν_7	230	0	4	0.75	216		$54S_8$, $14S_{11}$	$\delta_{as}SiCl_3$
ν_8	203	10	2	0.75	193		$20S_7$, $74S_9$	$\delta_{as}SiCl_3$
ν_9	150	0.4	2	0.69	142		$10S_2$, $46S_7$, $23S_9$, $12S_{10}$	$\delta_s SiCl_3$
ν_{10}	133	0	3	0.74	124		$44S_8$, $35S_{10}$, $53S_{11}$	$\rho SiCl_3$
ν_{11}	73	1	0.3	0.74	67		$61S_6$, $22S_{10}$, $13S_{11}$	δNSi_2
ν_{12}	24	0	0	0.56	22		$106S_{12}$	$\tau SiCl_3$
B								
ν_{13}	1175	669	0.2		1087	1074	$81S_{13}$, $31S_{17}$	$\nu_{as}NSi_2$
ν_{14}	877	86	0		788	786[l]	$24S_{13}$, $65S_{17}$	$\delta_{\parallel}$ND
ν_{15}	667	551	1		621	612	$31S_{14}$, $60S_{16}$	$\nu_{as}SiCl_3$
ν_{16}	631	72	4		590	590	$35S_{14}$, $68S_{15}$	$\nu_{as}SiCl_3$
ν_{17}	497	96	0.1		466	471	$30S_{14}$, $28S_{15}$, $31S_{16}$	$\nu_s SiCl_3$
ν_{18}	418	33	1		371	367	$37S_{18}$, $20S_{22}$, $40S_{23}$	cpld[j]
ν_{19}	267	41	1		252	250	$86S_{19}$	$\delta_s SiCl_3$
ν_{20}	242	1	0.4		210	208	$25S_{18}$, $28S_{21}$, $21S_{22}$	cpld[j]
ν_{21}	221	8	4		207		$29S_{18}$, $39S_{21}$	cpld[j]
ν_{22}	180	5	0.6		171		$92S_{20}$, $12S_{22}$, $12S_{23}$	$\delta_{as}SiCl_3$
ν_{23}	127	1	1		117		$26S_{18}$, $34S_{21}$, $40S_{22}$, $52S_{23}$	$\rho SiCl_3$
ν_{24}	24	1	0.1		22		$11S_{21}$, $35S_{22}$, $17S_{23}$, $152S_{24}$	$\tau SiCl_3$

[a] Unscaled frequency (cm^{-1}) from the HF/6-31G* calculation. [b] Infrared intensity (km mol^{-1}). [c] Raman scattering activity ($Å^4$ amu^{-1}). [d] Depolarization factor. These are all 0.75 for the B modes. [e] Frequency (cm^{-1}) after scaling. [f] Frequency observed in ref 15. [g] Potential energy distribution: terms ≥10%. [h] Infrared. [i] Raman. [j] Modes strongly coupled. [k] Average of infrared (128 cm^{-1}) and Raman (132 cm^{-1}) frequencies. [l] Reference 15 has 786 cm^{-1} in Table 5 and 796 cm^{-1} in Table 1.

To predict where the δNH bending modes would appear in the spectrum, NH−ND frequency shifts were calculated; these are listed in the sixth column of Table 7.

Many of the frequencies appear in A/B pairs, as occurred also for the $SiCl_3$ compound, and the broad bands observed in the liquid-phase spectra are clearly composite. Refinement of scale factors for the HF/6-31G* force constants had to be limited to three parameters, those for the νNH and ν_{as}NSi stretches and that for the $\delta_{\parallel}$NH motion.The remaining scale factors were transferred from $NH(SiCl_3)_2$ or $SiHMe_3$.[23] (The symmetry coordinates for the latter provided the basis for all those for the disilazane except for those involving the $HNSi_2$ system, which were as for the $SiCl_3$ compound.) Insofar as the $SiHMe_3$ methyl rocking coordinates ρMe were based on motions A′ and A″ with respect to the local symmetry of the methyl group, as in the case of trimethylamine,[31] a number of the methyl rocking motions in the disilazane could be categorized as either ρ' or ρ'' motions. The high degree of coupling in most cases meant

TABLE 3: Symmetry Coordinates and Scale Factors for $NH(SiCl_3)_2$[a]

motion	symmetry coordinate[b]	scale factor[c]
νNH	$S_1 = r_4$	0.8027(281)
$\nu_s NSi_2$	$S_2 = r_2 + r_3$	0.9396(358)
$\nu_{as} NSi_2$	$S_{13} = r_2 - r_3$	0.9121(326)
νSiCl	S_3, $S_{14} = r_5 \pm r_8$	0.8792(141)
νSiCl	S_4, $S_{15} = r_6 \pm r_9$	0.8792(141)
νSiCl	S_5, $S_{15} = r_7 \pm r_{10}$	0.8792(141)
δNSi_2	$S_6 = 2\gamma_{2,3} - \gamma_{2,4} - \gamma_{3,4}$	0.8470[d]
$\delta_s SiCl_3$	$S_7, S_{19} = (\alpha_{5,6} + \alpha_{5,7} + \alpha_{6,7}) \pm (\alpha_{8,9} + \alpha_{8,10} + \alpha_{9,10})$	0.9026(162)
$\delta_{as} SiCl_3$	S_8, $S_{20} = (2\alpha_{5,6} - \alpha_{5,7} - \alpha_{6,7}) \pm (2\alpha_{8,9} - \alpha_{8,10} - \alpha_{9,10})$	0.9026(162)
$\delta_{as} SiCl_3$	S_9, $S_{21} = (\alpha_{5,7} - \alpha_{6,7}) \pm (\alpha_{8,10} - \alpha_{9,10})$	0.9026(162)
$\rho SiCl_3$	$S_{10}, S_{22} = (2\beta_{2,5} - \beta_{2,6} - \beta_{2,7}) \pm (2\beta_{3,8} - \beta_{3,9} - \beta_{3,10})$	0.8460[e]
$\rho SiCl_3$	S_{11}, $S_{23} = (\beta_{2,6} - \beta_{2,7}) \pm (\beta_{3,9} - \beta_{3,10})$	0.8460[e]
$\tau SiCl_3$	S_{12}, $S_{24} = (\tau_{3,5} + \tau_{3,6} + \tau_{3,7}) \pm (\tau_{2,8} + \tau_{2,9} + \tau_{2,10})$	0.8460[e]
$\delta_{\parallel}$NH	$S_{17} = \gamma_{2,4} - \gamma_{3,4}$	0.7545(279)
$\delta_{\perp}$NH	$S_{18} = w_{1,2,3,4}$	0.6652(436)

[a] In the C_2 point group, S_1-S_{12} (positive sign alternative) belong to the A symmetry species and $S_{13}-S_{24}$ to the *B* species (negative sign alternative). Normalization factors omitted. [b] Internal coordinates as defined in Table 1. [c] In parentheses, the standard error in the last digits quoted. [d] Transferred from $NMe(SiH_3)_2$ (current work in our laboratories). [e] Transferred from SiH_3SiHCl_2[22] after squaring to allow for a redefinition.

TABLE 4: Symmetry Force Constants of the Scaled HF/6-31G* Force Field for $NH(SiCl_3)_2$[a]

Symmetry Species A

6.2552								
0.0673	4.9577							
−0.0074	0.0968	3.1275						
−0.0396	0.1438	0.1605	3.0776					
−0.0078	0.1058	0.2028	0.1898	3.0559				
−0.0919	0.1874	−0.0018	0.0179	0.0076	0.4495			
0.0509	−0.3394	0.0899	0.0684	0.1205	−0.0763	2.0369		
0.0047	−0.0002	0.0979	0.0870	−0.2203	−0.0244	−0.0318	0.8186	
0.0049	0.0246	0.1643	−0.1782	−0.0058	0.0093	−0.0144	−0.0165	0.8824
0.0411	0.0424	0.2136	−0.1299	−0.1126	0.0111	−0.0232	0.0490	0.1866
	0.8454							
−0.0485	−0.0066	0.0213	0.2248	−0.1826	−0.0107	−0.0049	0.1675	−0.1069
	−0.0895	0.8194						
0.0065	−0.0028	−0.0078	0.0057	0.0055	0.0141	−0.0026	−0.0116	0.0256
	−0.0006	0.0197	0.0363					

Symmetry Species B

4.1424								
0.2396	3.0862							
0.2275	0.1452	3.0265						
0.2549	0.1429	0.1522	3.0342					
0.1568	0.0341	0.0053	0.0147	0.3814				
−0.0268	−0.0488	−0.0037	0.0336	−0.0008	0.0884			
−0.05140	0.1731	0.1364	0.2022	−0.0351	0.0259	1.8275		
0.0563	0.0729	0.0778	−0.1986	−0.0022	0.0195	−0.0442	0.8054	
−0.0316	0.1966	−0.1900	0.0017	0.0302	0.0405	0.0091	−0.0015	0.8545
−0.0487	0.2205	−0.1410	−0.0798	0.0721	−0.0817	0.0193	0.1117	0.0954
	0.7703							
−0.0063	−0.0343	0.2134	−0.1550	−0.0469	0.0182	−0.0332	0.1615	−0.0924
	0.0007	0.7848						
−0.0055	−0.0165	0.0049	0.0036	0.0002	0.0035	0.0055	0.0122	0.0105
	−0.0187	0.0298	0.0059					

[a] Units: aJ Å^{-2}, aJ Å^{-1} rad^{-1}, aJ rad^{-2}.

that only a qualitative description of each mode was appropriate for inclusion in Table 7.

This coupling extends also to the $\nu_s NSi_2$ motion. However, the mode with the highest PED contribution from the $\nu_s NSi_2$ force constant, at 570 cm^{-1}, is well reproduced by the scale factor transferred from $NH(SiCl_3)_2$ and there is no evidence for significant error in this factor.

A surprising feature was the absence of any mode specifically associated with the $\delta_{\perp}$NH motion, the PED terms being distributed over a series of frequencies from 350 cm^{-1} downward. This is due to an unusually low force constant for this motion. A more detailed investigation of the far-infrared spectrum is desirable.

$NH(SiHCl_2)_2$. *General Assignments*. The first consideration here is to inquire if existing vibrational spectra are compatible with the presence of two conformers, as the ab initio study suggested.[11] The second line of inquiry will be into the conformational dependences of the SiH stretching frequency and SiH and SiCl properties generally.

Table 8 shows the ab initio data obtained for the two structures **I** and **II**, which represent minima on the PE surface at the HF/6-31G* level, the HSiNH dihedral angles for which are 171.5°,171.5° (C_2) and 0°,180° (C_s), respectively. The frequencies include those calculated before and after scaling of the force constants involved, together with a provisional assignment of those previously observed.[21]

TABLE 5: Valence Force Constants and SiCl Bond Properties from the Scaled HF/6-31G* Force Field for $NH(SiCl_3)_2$

A. Diagonal Valence Constants and α Interactions

constant[a]	f	f_{emp}[b]	constant[a]	f	f_{emp}[b]
f(NSi)	4.5500	4.53	$f'(NSi_2,NSi_3)$	0.4077	0.13
$f(Si_2Cl_5)$, $f(Si_3Cl_8)$	3.1070	3.00	$f'(Si_2Cl_5,Si_3Cl_6)$	0.1528	0.20
$f(Si_2Cl_6)$, $f(Si_3Cl_9)$	3.0522	3.00	$f'(Si_2Cl_5,Si_3Cl_7)$	0.1729	0.20
$f(Si_2Cl_7)$, $f(Si_3Cl_{10})$	3.0452	3.00	$f'(Si_2Cl_6,Si_3Cl_7)$	0.1710	0.20

B. Remote Valence Interaction Constants

stretch−stretch constant	f'[a]	$\langle Cl_iSi_2Si_3Cl_j$/deg	rCl_iCl_j/Å
$f'(Si_2Cl_5,Si_3Cl_{10})$, $f'(Si_2Cl_7,Si_3Cl_8)$	0.0300	−41.87	4.125
$f'(Si_2Cl_6,Si_3Cl_9)$	0.0256	−56.41	5.851
$f'(Si_2Cl_5,Si_3Cl_8)$	0.0206	68.21	4.010
$f'(Si_2Cl_6,Si_3Cl_{10})$, $f'(Si_2Cl_7,Si_3Cl_9)$	0.0188	75.82	5.504
$f'(Si_2Cl_7,Si_3Cl_{10})$	0.0108	−151.95	5.816
$f'(Si_2Cl_5, Si_3Cl_9)$, $f'(Si_2Cl_6, Si_3Cl_8)$	0.0076	−174.10	5.769

C. Electrical Properties Associated with the SiCl Bonds

bond	$\partial\boldsymbol{\mu}/\partial r$[c]/e	ϕ[d]/deg	ξ[e]/e	q[f]/e
Si_2Cl_5	−1.012	1.8	1.139	−0.257
Si_2Cl_6	−1.116	1.2	1.231	−0.274
Si_2Cl_7	−1.089	2.7	1.209	−0.253

[a] Units: aJ Å^{-2}. [b] Empirical force field of ref 15. [c] Dipole derivative with respect to stretching of the SiCl bond. [d] Angle between $\partial\boldsymbol{\mu}/\partial r$ and the bond direction. [e] King effective atomic charge on Cl. [f] Mulliken atomic charge on Cl.

Scaling was carried out in part by transfer of scale factors from a parallel HF/6-31G* treatment of $NMe(SiH_3)_2$ and a similar one of SiH_3SiHCl_2[22] and in part by refinement to eight observed frequencies, four of which, 3393, 2247, 1192, and 964 cm^{-1}, are common to both structures and are of uncontroversial origin.

Of the other four frequencies, two, at 460 and 390 cm^{-1}, represent the principal change in assignment made here from those of Fleischer et al.[21] Whereas previously the $\delta_\perp$NH mode was estimated to lie at 964 cm^{-1}, not far below the in-plane mode at 1192 cm^{-1}, the unscaled HF/6-31G* calculations place these two modes at 533 and 1364 cm^{-1} in **I** and 449 and 1364 cm^{-1} in **II**. Two previously unaccounted-for bands at 460 and 390 cm^{-1} are then readily explained on the basis of scale factors which resemble closely those for the in-plane $\delta_{||}$NH motion, as shown in Table 9. These two bands thus constitute strong evidence for the presence of two distinct conformers.

The number of polarized Raman lines below 500 cm^{-1} also is better explained by the presence of both **I** and **II**, as shown in Table 8. An additional very weak polarized Raman line at 763 cm^{-1}, previously assigned as the combination 501 + 262 cm^{-1}, then becomes a fundamental, the $\nu_s NSi_2$ mode for **I**, 57 cm^{-1} higher than its value for **II**, as predicted for both the unscaled and scaled values.

We note also that if our interpretation of the spectra below 510 cm^{-1} is correct, the frequencies 501 and 262 cm^{-1} are associated with different conformers and cannot therefore give rise to a combination band.

As might be expected, the four δSiH modes, once scaled, are little different for the two conformers and do not assist in discriminating between them. The highest unscaled δSiH differs by 21 cm^{-1} for **I** and **II**, which arises from the coupling in **II** which occurs with this mode and $\nu_{as}NSi_2$ above. This coupling largely disappears on scaling since the scale factors for the two kinds of motion are very different, as seen in Table 9.

Only one of the νSiCl modes, the lowest one near 500 cm^{-1}, is significantly different for the two conformers.

Overall, the evidence for two distinct conformations appears strong, which is perhaps surprising in view of the flat nature of the PE surface according to both HF and MP2 calculations,[11] which is reflected in the very low frequencies predicted at the bottom end of the spectrum. The lowest two of these are largely torsions of the $SiHCl_2$ groups but involve also a significant amount of other kinds of motion.

TABLE 6: Comparison of ab Initio and Experimental Geometries for $NH(SiMe_3)_2$

length/angle[a]	HF/6-31G*	MP2/6-31G*	obs[b]	angle	HF/6-31G*	MP2/6-31G*	obs[b]
rNH	1.0024	1.0177	(0.98)	$\angle Si_3C_5H_{11}$	111.3	111.1	111.2(8)
rNSi	1.7432	1.7532	1.738(5)	$\angle Si_3C_5H_{12}$	110.7	110.8	"
rSi_3C_5	1.8900	1.8847	1.876(1)	$\angle Si_3C_5H_{13}$	112.4	112.0	"
rSi_3C_6	1.8903	1.8844	"	$\angle H_{11}C_5H_{12}$	107.6	108.0	−
rSi_3C_7	1.8915	1.8864	"	$\angle H_{11}C_5H_{13}$	107.6	107.8	−
rC_5H_{11}	1.0867	1.0941	1.104(3)	$\angle H_{12}C_5H_{13}$	107.0	107.1	−
rC_5H_{12}	1.0878	1.0953	"	$\angle Si_3C_6H_{14}$	111.7	111.5	111.2
rC_5H_{13}	1.0873	1.0948	"	$\angle Si_3C_6H_{15}$	111.2	111.0	"
rC_6H_{14}	1.0881	1.0952	"	$\angle Si_3C_6H_{16}$	111.5	111.3	"
rC_6H_{15}	1.0873	1.0947	"	$\angle H_{14}C_6H_{15}$	107.1	107.3	−
rC_6H_{16}	1.0871	1.0942	"	$\angle H_{14}C_6H_{16}$	107.6	107.9	−
rC_7H_{17}	1.0871	1.0943	"	$\angle H_{15}C_6H_{16}$	107.5	107.8	−
rC_7H_{18}	1.0881	1.0955	"	$\angle Si_3C_7H_{17}$	111.7	111.2	111.2
rC_7H_{19}	1.0874	1.0945	"	$\angle Si_3C_7H_{18}$	111.4	111.3	"
$\angle$SiNSi	134.4	131.4	131.5(15)	$\angle Si_3C_7H_{19}$	111.2	111.1	"
$\angle N_1Si_3C_5$	110.6	109.9	110.7(5)[c]	$\angle H_{17}C_7H_{18}$	107.4	107.7	−
$\angle N_1Si_3C_6$	107.2	107.3	"	$\angle H_{17}C_7H_{19}$	107.3	107.6	−
$\angle N_1Si_3C_7$	112.0	112.2	"	$\angle H_{18}C_7H_{19}$	107.5	107.8	−
$\angle C_5Si_3C_6$	109.8	110.0	−	$\langle C_6Si_3N_1H_2$	−19.3[e]	−19.4[e]	−13(4)[d,e]
$\angle C_5Si_3C_7$	108.4	108.5	−	$\langle C_9Si_4N_1H_2$	−19.3[e]	−19.4[e]	−37(3)[d,e]
$\angle C_6Si_3C_7$	108.7	108.9	−	$\langle C_6Si_3Si_4C_9$	−47.6[e]	−48.8[e]	−
				$\langle H_{12}C_5Si_3N_1$	179.1	179.6	161(6)[d]
				$\langle H_{15}C_6Si_3N_1$	179.1	179.1	"
				$\langle H_{18}C_7Si_3N_1$	−177.9	−178.7	"

[a] Atom numbering as in Figure 1. Bond lengths in angstroms; angles in degrees. [b] Constraints in the ED model: planarity of the HNSiSi skeleton; $\angle HNSi_3 = \angle HNSi_4$; $rNSi_3 = rNSi_4$; local C_{3v} symmetry for the $SiMe_3$ groups, plus a tilt (found to be 2.4(9)°); local C_{3v} symmetry for the CH_3 groups with axis coincident with the SiC direction; equal twisting of the methyl groups from the fully staggered position.[6] [c] Average value. [d] Redefined to represent a conventional dihedral angle. [e] The corresponding angles in the ED C_2 structure of $NMe(SiMe_3)_2$ were −34.4, −34.3, and −87.5°, respectively.[9]

TABLE 7: Comparison of ab Initio and Mean Observed Vibrational Data for $NH(SiMe_3)_2$, Omitting CH_3 Stretches and Deformations

mode/sym	ν_{unsc}[a]	A[b]	R[c]	ν_{sc}[a]	$\Delta\nu$[d]	ν_{obs}	composition[e]
ν_1 A	3771	19	56	3378	908	3378 IR[f−i]	νNH
ν_{58} B	1338	277	0	1180	129	1180 IR[f−i]	δ_{ll}NH, $\nu_{as}NSi_2$
ν_{20} A	992	83	1	904	2	−	ρ''Me, ν_sNSi_2
ν_{59} B	987	515	0	932	58	932 IR[f,g,i]	$\nu_{as}NSi_2$, ρ''Me, δ_{ll}NH
ν_{21} A	956	168	3	879	0	887 IR,R[f−h]	ρ''Me
ν_{60} B	947	222	0	874	7	...	ρ'Me, δ_{as}Me, $\nu_{as}SiC_3$
ν_{22} A	938	0	4	863	0	−	ρ'Me
ν_{61} B	934	28	3	856	18	848 IR[g]	ρ'Me, $\delta_{as}SiC_3$, ρ''Me
ν_{62} B	929	65	2	831	48	836 IR,R[f−h]	ρ''Me
ν_{23} A	871	36	3	792	2	771 IR[f,h]	ρ''Me
ν_{63} B	843	42	0	765	0	756 IR[f,g]	ρ''Me, ρ'Me, $\nu_{as}SiC_3$
ν_{24} A	834	0	4	757	0	746 R[f−h]	ρ''Me, $\nu_{as}SiC_3$, ρ'Me
ν_{64} B	823	4	1	749	44	749 IR[h]	$\nu_{as}SiC_3$, ρ''Me, ρ'Me
ν_{25} A	749	0	0	699	1	−	ρ'Me
ν_{65} B	747	0	0	691	1	−	$\nu_{as}SiC_3$, ρ''Me, ρ'Me
ν_{26} A	733	26	3	687	0	686 IR[f−,i]	$\nu_{as}SiC_3$, ρ'Me, ρ'Me
ν_{66} B	730	9	11	689	0	685 R[f−h]	$\nu_{as}SiC_3$, ρ''Me, ρ'Me
ν_{67} B	726	38	4	651	0	663? IR[f]	ρ''Me, ρ'Me
ν_{27} A	724	0	8	676	1	−	ρ''Me, ν_sSiC_3
ν_{28} A	710	3	11	653	0	669 R?[f,h]	ρ''Me, ρ'Me
ν_{68} B	638	8	1	626	3	619 IR[f−h]	ν_sSiC_3, ρ''Me
ν_{29} A	588	5	28	568	7	570 IR,R[f−i]	ν_sSiC_3, ν_sNSi_2
ν_{69} B	373	72	0	350	1	∼350 IR[j]	ρSiC_3, $\delta_\perp$NH, ρ''Me, ρ'Me
ν_{30} A	366	3	3	351	2	349 R[f−j]	ρ''Me, δ_sSiC_3, δ_sNSi_2, ν_sNSi_2
ν_{70} B	293	9	1	260	5	−	ρ''Me, $\delta_{as}SiC_3$, δ_sSiC_3, $\delta_\perp$NH, ρSiC_3
ν_{71} B	263	13	0	250	13	245 IR[j]	ρ''Me, ρSiC_3, ρ'Me
ν_{31} A	252	0	1	245	0	248 R[f−h]	$\delta_{as}SiC_3$, ρSiC_3, ρ'Me
ν_{72} B	242	6	1	233	28	231 R[f]	$\delta_{as}SiC_3$, ρ''Me, δ_sSiC_3, ρ'Me, $\delta_\perp$NH
ν_{32} A	225	3	0	219	0	217 R[f]	$\delta_{as}SiC_3$, ρ''Me, δ_sSiC_3, ρ'Me
ν_{73} B	207	0	0	201	0	−	$\delta_{as}SiC_3$, ρ'Me, ρSiC_3
ν_{33} A	192	0	1	186	0	196 R[f,g]	$\delta_{as}SiC_3$, ρ''Me, δ_5SiC_3, ρSiC_3
ν_{74} B	182	0	0	181	2	−	τMe
ν_{34} A	180	0	1	177	0	174 R[f−h]	$\delta_{as}SiC_3$, τMe, ρSiC_3
ν_{35} A	172	0	0	171	0	−	τMe
ν_{75} B	171	0	0	170	1	−	τMe
ν_{36} A	170	0	1	167	0		$\delta_{as}SiC_3$, ρSiC_3, τMe
ν_{76} B	165	2	1	159	7		$\delta_{as}SiC_3$, ρSiC_3, ρ''Me
ν_{37} A	156	0	0	156	0		τMe
ν_{77} B	152	0	0	152	4	146 R[f]	τMe
ν_{38} A	100	0	0	94	0		δNSi_2, ρSiC_3
ν_{78} B	36	0	0	36	2		τCSiNSi, ρSiC_3, $\delta_\perp$NH, $\delta_{as}SiC_3$
ν_{39} A	36	0	0	36	0		τCSiNSi

[a] Unscaled and scaled frequencies (cm^{-1}) from the HF/6-31G* force field. [b] Infrared intensity in km mol^{-1}. [c] Raman scattering activity in $Å^4$ amu^{-1}. [d] Frequency shift due to deuterium substitution on nitrogen. [e] In order of decreasing importance in the potential energy distribution. [f] Reference 16. [g] Reference 17. [h] Reference 18. [i] Reference 19. [j] Reference 20.

The six scale factors in Table 9 which were determined independently for each of the two conformers would in general be expected to be very similar, if not identical. That only in one case, the factor for ν_sNSi_2, does the difference between the two conformers lie very slightly outside the combined standard errors is an effective demonstration of the correctness of our assignments.

SiH Bonds and the νSiH Region. Table 10 shows data relating to the SiH bond and the hydrogen atom in it for eight structures, only two of which, **II** and **III**, are equilibrium ones. An HNSiH angle of 90° indicates an SiH bond at right angles to the skeletal plane. The 90°,90° structure **VII** has the SiH bonds on opposite sides of this plane (C_2) while the 90°,−90° structure **VIII** has its SiH bonds on the same side (C_s). The C_{2v} structures **IV** (180°,180°) and **IX** (0°,0°) have in-plane SiH bonds respectively adjacent to and remote from each other.

The unscaled vibration frequencies ν_2 and ν_3 and their accompanying infrared intensities A_2 and A_3 refer to the normal modes of the molecule and only come to equal the isolated frequencies ν^{is}SiH associated with individual SiH bonds when the two SiH bond stretches are completely decoupled in the d_0 isotopomer. The ν^{is}SiH values were calculated ab initio for the species $NH(SiHCl_2)(SiDCl_2)$ in all the structures except for **V** and **VI**, where recourse had to be made to a harmonic local mode treatment of the d_0 data.[22]

A problem immediately arises in that, for both of the conformers identified as being present from the lower part of the spectrum, there should be a significant splitting seen in the νSiH region, either 12.5 cm^{-1} for the 180°,180° structure **IV** or 19.2 cm^{-1} for the 0°,180° one, **II**, at the HF level. A single MP2 calculation for the 180°,180° conformer **III** suggests that at this level the splitting will be slightly less. However, only a single band is in fact observed, either in the infrared spectrum of the gas, as in Figure 2a, or in the Raman effect in the liquid phase, as in Figure 2b.[21]

The Raman band is well fitted by a single Lorentzian profile. Superimposed on the infrared band is a spectrum predicted from the ab initio data above. For each of the four component bands predicted, we have assumed a Lorentzian profile and an arbitrary constant width at half-height of 6.7 cm^{-1}. The peak frequencies of each transition were scaled with a mean scale factor, while the relative HF/6-31G* intensities were left unchanged. (For

TABLE 8: Comparison of ab Initio and Observed Vibrational Data for Two Conformers of $NH(SiHCl_2)_2$

	I, C_2 (171.5°,171.5°)				**II**, C_s (0°,180°)						
	ν_{unsc}[a]	A[b]	ν_{sc}[c]	ν_{obs}[d]	ν_{unsc}[a]	A[b]	R[e]	dp[f]	ν_{sc}[c]	ν_{obs}[d]	motion
ν_1	3741 A	72	3393	3393 s[g]	3749	76	60	0.28	3393	3393 s[g]	νNH
ν_2	2508 A	209	2252	2247 vs[g]	2512	100	84	0.15	2256	2247 vs[g]	νSiH
ν_3	2496 B	9	2242	2247 vs[g]	2493	140	127	0.16	2238	2247 vs[g]	νSiH
ν_4	1364 B	450	1192	1192 vs[g]	1364	301	0.5	0.74	1192	1192 vs[g]	$\delta_{\parallel}$NH
ν_5	1009 B	448	964	964 vs[g]	1009	293	1	0.71	964	964 vs[g]	$\nu_{as}NSi_2$
ν_6	973 A	11	886	~890 sh[h]	952	464	7	0.63	875	860 sh	δSiH
ν_7	911 B	384	831	827 vs	920	41	6	0.60	838		δSiH
ν_8	886 A	10	808		902	464	3	0.75	822	827 vs	δSiH
ν_9	875 B	301	796	815 sh	889	5	14	0.75	810	797 w, dp	δSiH
ν_{10}	806 A	45	763	763 vw, p[g,i]	743	79	5	0.67	706	706 w, p[g]	ν_sNSi_2
ν_{11}	644 B	512	590	594 vs	632	421	2	0.75	587	594 vs	$\nu_{as}SiCl_2$
ν_{12}	611 A	17	572	570 w, dp	606	2	6	0.75	568	570 w, dp	$\nu_{as}SiCl_2$
ν_{13}	585 A	55	545		574	93	7	0.25	536		ν_sSiCl_2
ν_{14}	547 B	119	510	525 s	528	25	12	0.05	495	501 vs, p	ν_sSiCl_2
ν_{15}	533 B	26	460	460 vw[g]	449	28	0.1	0.75	390	390 vw[g]	$\delta_{\perp}$NH
ν_{16}	297 B	13	273		386	43	2	0.41	358	346 w, p	δ_{skel}
ν_{17}	287 A	4	267	262 m, p	286	2	1	0.75	259		δ_{skel}
ν_{18}	221 B	6	200	190 sh, dp	254	2	5	0.49	234	235 m, p	δ_{skel}
ν_{19}	204 B	15	186	190 sh, dp	207	14	0.5	0.71	191	190 sh, dp	δ_{skel}
ν_{20}	174 A	2	161	174 w, dp	180	10	3	0.74	166	174 w, dp	δ_{skel}
ν_{21}	147 A	0	135	143 s, dp	143	1	3	0.75	132	143 s, dp	δ_{skel}
ν_{22}	123 A	10	113		91	3	0.4	0.68	84	88 sh, dp	δ_{skel}
ν_{23}	17 B	2	17		20	1	0.1	0.75	20		τ_{skel}
ν_{24}	6 A	0	6		17	0	0.2	0.75	17		τ_{skel}

[a] Unscaled frequency in cm^{-1} from the HF/6-31G* calculation. Symmetry species A and B are specified for the C_2 structure. A″ modes for the C_s structure are identified by depolarization ratios of 0.75. [b] Calculated infrared intensity in km mol^{-1}. [c] Frequency after scaling (see text). [d] Frequencies reported in ref 21. Raman data, measured in the liquid phase, are identified by p (=polarized) or dp (=depolarized). All other data are infrared. [e] Calculated Raman scattering activity in $Å^4$ amu^{-1}. [f] Depolarization ratio. [g] Frequency used in refining scale factors. [h] Seen in Figure 1 of ref 21 but not tabulated. [i] This frequency was previously assigned to the combination 262 + 501 cm^{-1}.[21]

TABLE 9: Scale Factors for Two Conformers of $NH(SiHCl_2)_2$

coordinate type[a]	**I** (C_2)	**II** (C_s)
νNH	0.8225(55)	0.8189(89)
ν_sNSi_2	0.9125(81)	0.9418(176)
$\nu_{as}NSi_2$	0.9507(96)	0.9658(195)
νSiH	0.8066(38)	0.8063(62)
νSiCl[b]	0.8792	0.8792
δSiH[c]	0.8296	0.8296
δ_{skel}[c]	0.8460	0.8460
τ_{skel}	1.0000	1.0000
δNSi_2[d]	0.8470	0.8470
$\delta_{\parallel}$NH	0.7307(78)	0.7193(155)
$\delta_{\perp}$NH	0.6965(65)	0.7036(127)

[a] As recommended in ref 28, apart from the skeletal torsions, which used the HSiNSi and ClSiNSi dihedral.angles. [b] Transferred from $NH(SiCl_3)_2$. [c] Transferred after squaring from SiH_3SiHCl_2.[22] [d] Transferred from $NMe(SiH_3)_2$ (current work in our laboratories).

comparison with the observed spectrum in Figure 2a, the total integrated area of the four predicted bands was equated to that of the single observed band.) However, the conformer abundancies were those given by the MP2 calculations, 43% (**IV**) and 57% (**II**), respectively.[11]

The inference is clear. On the basis of the ab initio evidence, we ought to be seeing a splitting into at least two bands, or at least a marked asymmetry. Failure to observe such a contour implies an additional broadening mechanism which is most likely to be a signal averaging on the time scale of the infrared vibrations due to the rapid interconversion of the two conformers.

If signal averaging is the appropriate explanation for this νSiH band, and by implication for other $NH(SiHR'R)_2$ compounds which exhibit only a single band, then we must suppose that the absence of such averaging in the modes below 1000 cm^{-1} is to be attributed to their greater separation for the two conformers.

When the sources of the calculated splittings are examined, these are seen to be two-fold: coupling between SiH bonds of identical strength, when these are oriented roughly parallel to each other, and a difference in strength, when the two bonds lie at differing torsional angles.

The presence or absence of coupling is best measured by the valence interaction constant f' which is clearly trivial in all cases except that in which the bonds are parallel. The source of this coupling seems very likely to lie in a dipole−dipole interaction.[13,24]

We now look again at the ν^{is}SiH values for $NH(SiHCl_2)_2$ in Table 10 and reassemble them differently in Table 11 together with the associated electrical properties, to see what may be learned generally about the effects of orientation.

The highest values of ν^{is}SiH occur for a bond with $\tau_i = 180°$, lying in the skeletal plane, while the lowest one is found with $\tau_i = 90°$. This is in accordance with an n(N)−σ*(Si−H) orbital interaction which weakens the SiH bond most when τ(H−N−Si−H) is 90°. However all the ν^{is}SiH values are sensitive to the orientation of the other SiH bond (SiH_j), extreme values differing by about 17−18 cm^{-1} ($\tau_i = 180,90°$) or 7.7 cm^{-1} ($\tau_i = 0°$). The smaller value for the latter is not surprising, since with $\tau_i = 0°$, the SiH_i bond is as remote from the other $SiHCl_2$ group as it can be. As mentioned above, in the 90°,90° structure **VII** the two SiH bonds lie on opposite sides of the skeletal plane, antiparallel to each other and therefore opposite SiCl bonds in the other group. In the 90°,−90° form **VIII**, the two SiH bonds are roughly parallel to each other.

In a search for correlations between ν^{is}SiH and the other properties listed in Table 11, the only one obvious is that with the sum of the Mulliken charges on the two chlorine atoms attached to the same silicon. This is shown in Figure 3 for the three types of SiH_i bond studied. While a connection is clear, although the gradient is different for each type of atom, its source remains a puzzle.

TABLE 10: Ab Initio Data for SiH Bonds in $NH(SiHCl_2)_2$ Structures

	structure							
	III$_{MP2}$	**IV**$_{HF}$	**II**$_{HF}$	**V**$_{HF}$	**VI**$_{HF}$	**VII**$_{HF}$	**VIII**$_{HF}$	**IX**$_{HF}$
τ_1,τ_2/deg[a]	180,180	180,180[b]	0,180	90,180[b]	0,90[b]	90,90[b]	90,−90[b]	0,0[b]
ΔE/H[c]	1.04534	0.22499	0.22419	0.22346	0.22145	0.22233	0.21888	0.22007
rSiH$_1$/Å	1.4695	1.4548	1.4564	1.4565	1.4570	1.4554	1.4580	1.4574
rSiH$_2$/Å	1.4695	1.4548	1.4537	1.4523	1.4563	1.4554	1.4580	1.4574
$\nu_2(d_0)$/cm^{-1}	2408.39	2509.11	2511.99	2520.23	2489.48	2495.15	2479.95	2486.52
$\nu_3(d_0)$/cm^{-1}	2397.25	2496.65	2492.77	2487.23	2487.37	2494.88	2474.58	2483.58
$\nu_2-\nu_3$/cm^{-1}	11.1	12.5	19.2	33.0	2.1	0.3	5.4	2.9
$\nu^{is}(1)$/cm^{-1} [d]	2402.85	2502.92	2492.77	2487.25[e]	2489.12[e]	2495.0	2477.26	2485.05
$\nu^{is}(2)$/cm^{-1} [d]	2402.85	2502.92	2511.99	2520.21[e]	2487.73[e]	2495.0	2477.26	2485.05
A_2/km mol^{-1}	161	212	100	98	111	7	274	195
A_3/km mol^{-1}	5	5	140	139	165	249	21	108
f'_{full}/aJ Å^{-2}	0.0134	0.0155	0.00	0.0019	0.0019	0.0007	0.0055	0.0041
f'_{HLM}/aJ Å^{-2}	0.0153	0.0179	0.00	0.0027[e]	0.0023[e]	*f*	0.0076	0.0042
$\partial\boldsymbol{\mu}/\partial r(1)$/e	−0.253	−0.289	−0.375	−0.346	−0.341	−0.314	−0.342	−0.349
$\phi(1)$/deg[g]	3.1	3.5	0.4	1.6	1.7	1.8	1.2	2.0
$\xi(H_1)$/e[h]	0.529	0.586	0.621	0.600	0.604	0.607	0.632	0.605
$\partial\boldsymbol{\mu}/\partial r(2)$/e	−0.253	−0.289	−0.272	−0.268	−0.316	−0.314	−0.342	−0.349
$\phi(2)$/deg[g]	3.1	3.4	5.0	3.6	3.2	1.8	1.2	2.0
$\xi(H_2)$/e[h]	0.529	0.586	0.571	0.572	0.608	0.607	0.632	0.605
$q(H_1)$/e[i]	*f*	−0.1074	−0.1052	−0.1024	−0.1091	−0.0989	−0.1079	−0.1123
$q(Si_1)$/e[i]	*f*	1.0644	1.0720	1.0840	1.0716	1.0884	1.0770	1.0697
$q(Cl_{1a})$/e[i]	*f*	−0.3153	−0.3181	−0.3239	−0.3060	−0.3192	−0.3042	−0.3117
$q(Cl_{1b})$/e[i]	*f*	−0.3153	−0.3181	−0.3262	−0.3251	−0.3367	−0.3334	−0.3121
$q(H_2)$/e[i]	*f*	−0.1074	−0.1018	−0.0952	−0.0998	−0.0988	−0.1079	−0.1123
$q(Si_2)$/e[i]	*f*	1.0644	1.0713	1.0669	1.0818	1.0884	1.0770	1.0697
$q(Cl_{2a})$/e[i]	*f*	−0.3153	−0.3175	−0.3252	−0.3112	−0.3189	−0.3335	−0.3117
$q(Cl_{2b})$/e[i]	*f*	−0.3153	−0.3175	−0.3170	−0.3339	−0.3369	−0.3042	−0.3121

[a] τ_1 and τ_2 are the H_1Si_1NH and H_2Si_2NH dihedral angles, respectively. [b] Nonstationary point structure: lowest frequency imaginary. [c] Energy in hartrees = −2472 − ΔE. [d] In the species $NH(SiHCl_2)(SiDCl_2)$. [e] Estimate from harmonic local mode fit to HF/6-31G* full normal coordinates. [f] Not available. [g] Angle between $\partial\boldsymbol{\mu}/\partial r$ and the SiH bond. [h] King effective atomic charge. [i] Mulliken atomic charge. Cl_{1a} and Cl_{1b} are attached to Si_1, Cl_{2a} and Cl_{2b} to Si_2.

TABLE 11: Variations in SiH_i Bond and Atom Properties with Torsional Angles τ_i, τ_j in $SiH_i\cdots SiH_j$ Systems in $NH(SiHCl_2)_2$

parameter[a]	τ_i values/ deg	$\tau_j = 180°$	$\tau_j = 0°$	$\tau_j = 90°$	$\tau_j = -90°$ [b]
$\nu^{is}SiH_i$	180	2502.9	2512.0	2520.2	R
	0	2492.8	2485.1	2489.1	R
	90	2487.3	2487.7	2495.0	2477.3
$\partial\boldsymbol{\mu}/\partial r_i$	180	−0.289	−0.272	−0.268	R
	0	−0.375	−0.349	−0.341	R
	90	−0.346	−0.316	−0.314	−0.342
$\xi(H_i)$	180	0.586	0.571	0.572	R
	0	0.621	0.605	0.604	R
	90	0.600	0.608	0.607	0.632
$q(H_i)$	180	−0.107	−0.102	−0.095	R
	0	−0.105	−0.112	−0.109	R
	90	−0.102	−0.100	−0.099	−0.108
$q(Si_i)$	180	1.064	1.071	1.067	R
	0	1.072	1.070	1.072	R
	90	1.084	1.082	1.088	1.077
$\sum q(Cl_i)$[c]	180	−0.631	−0.635	−0.642	R
	0	−0.636	−0.624	−0.631	R
	90	−0.650	−0.645	−0.656	−0.638

[a] As defined in Table 10. Units: ν^{is}SiH in cm^{-1}; $\partial\boldsymbol{\mu}/\partial r$, ξ, and q in e. [b] R: repeats data for $\tau_j = 90°$. [c] $q(Cl_{ia}) + q(Cl_{ib})$.

Two further points may be made about these νSiH values. If we compare similar structures, e.g. **IV** for $NH(SiHCl_2)_2$ and **I** for $NMe(SiHCl_2)$,[23] our calculations predict only a small change in ν^{is}SiH of several cm^{-1}, which suggests that the chemical effect on the SiH bond of methyl substitution on nitrogen is negligible.

A second feature of these results is that the effect on νSiH of chlorine substitution on the silicon is greater, both experimentally and theoretically in our ab initio calculations, than would be expected from data for silanes. In the latter, replacement of methyl by chlorine raises ν^{is}SiH by about 44 cm^{-1},[14] whereas here we see experimentally an increase of 55 cm^{-1}, from $NH(SiHMeCl)_2$, at 2192 cm^{-1},[13] to $NH(SiHCl_2)_2$, at 2247 cm^{-1}.[21] The corresponding changes calculated ab initio for similar structures are about 60 cm^{-1}, in good agreement. A possible explanation involves an effect connected with the interaction between the chlorine nonbonding electrons and the nitrogen p_π electron system, which appears to be an important influence on the conformation.[12] If such be the case, similar larger enhancements of ν^{is}SiH should be found in molecules such as $NY_2SiHMeCl$ and NY_2SiHCl_2 (Y = H, Me). The connection noted above between ν^{is}SiH and the sum of the Mulliken charges on the chlorines might then be an associated symptom. However, a simpler explanation is that the simultaneous substitution in these disilazanes of a chlorine on the *remote* Si atom is through an inductive effect increasing the shift due to chlorine attaching to the *same* Si atom.

Examining the dipole derivatives $\partial\boldsymbol{\mu}/\partial r$(SiH), we find the lowest values for bonds with $\tau_i = 180°$ but there is no clear distinction between those for the 90° and 0° ones. There is no uniform connection between change in ν^{is}SiH and change in $\partial\boldsymbol{\mu}/\partial r$. Figure 4 shows a rough connection between $\partial\boldsymbol{\mu}/\partial r(SiH_i)$ and $H_iSiNH(C)$ torsional angle, which incorporates data for both $NH(SiHCl_2)_2$ and $NMe(SiHCl_2)_2$.[24]

The unsigned King effective charge ξ_H, which forms an overall measure of the contribution of the atom concerned to the intensities of all the vibrations and rotations of the molecule, follows the variations in $\partial\boldsymbol{\mu}/\partial r$(SiH) to a fair extent, which suggests that the SiH stretching intensity plays a dominant role in determining the value of ξ.

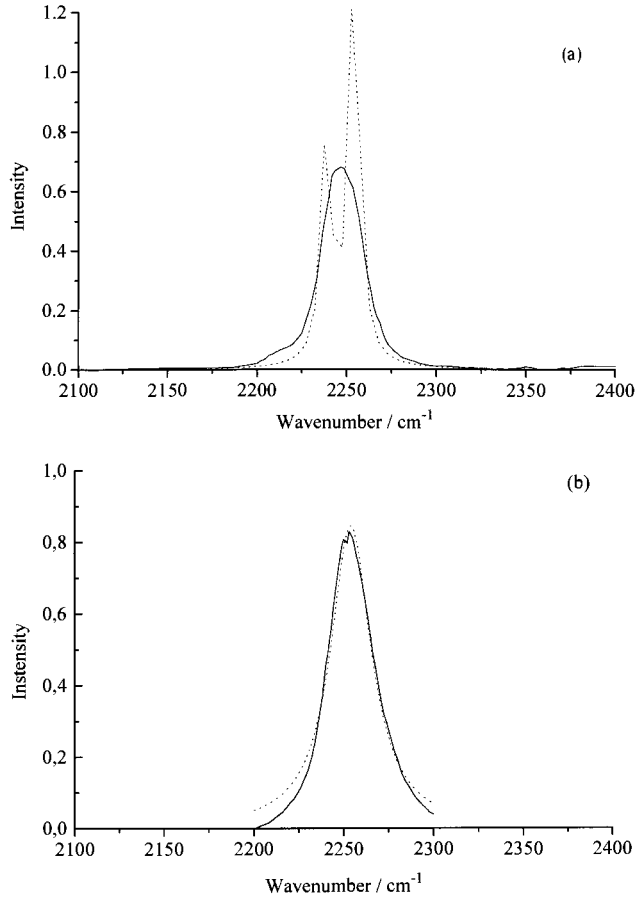

Figure 2. The νSiH band of $NH(SiHCl_2)_2$ conformers: (a) in the infrared spectrum (gas phase); (b) in the Raman spectrum (liquid phase), from the work described in ref 21. Superimposed on the infrared band is the spectrum (dotted) predicted from the four scaled HF/6-31G* frequencies, 2253.0 (**IV**), 2241.8 (**IV**), 2255.6 (**II**), and 2238.4 (**II**) cm^{-1} and their unscaled intensities, weighted by abundancies for the two conformers determined at the MP2/6-31G* level, of 91.2, 2.0, 56.9, and 79.7 km mol^{-1}, respectively. Each transition was represented by a Lorentzian shape with width at half-height of 6.7 cm^{-1}. The Raman band has a single Lorentzian profile superimposed, with a half-width of 27.5 cm^{-1}. The single Lorentzian band best fitting the infrared spectrum has a half-width of 23.4 cm^{-1}.

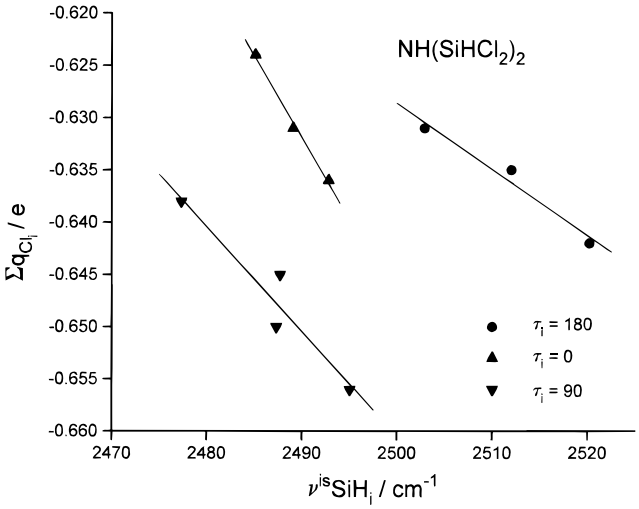

Figure 3. Correlation between ν^{is}SiH and $\sum q_{Cl}$ for $NH(SiHCl_2)_2$.

There is however no obvious correlation to be seen between the Mulliken atomic charge q and $\partial\boldsymbol{\mu}/\partial r$, from which we infer that the variations in the latter arise primarily from changes in the charge flux associated with stretching of the bond.[32]

A general feature of all the $NH(SiHCl_2)_2$ structures is the small deviation of the direction of the dipole derivative vector $\partial\boldsymbol{\mu}/\partial r$ from that of the SiH bond concerned. In this respect, $NH(SiHCl_2)_2$ follows other SiH compounds.[22−24]

SiCl Bond Properties. Table 12 shows some properties of the SiCl bonds in six of the structures studied. As in $NY(SiHMeCl)_2$ molecules,[13] the values of the valence interaction constant f' are surprisingly large for pairs of remote bonds. Included in this table are some geometric quantities which might be thought to be influencing f', namely, the DCl···Cl distances and the τCl_iSiNH and $\tau Cl_iSiSiCl_j$ torsional angles. No simple

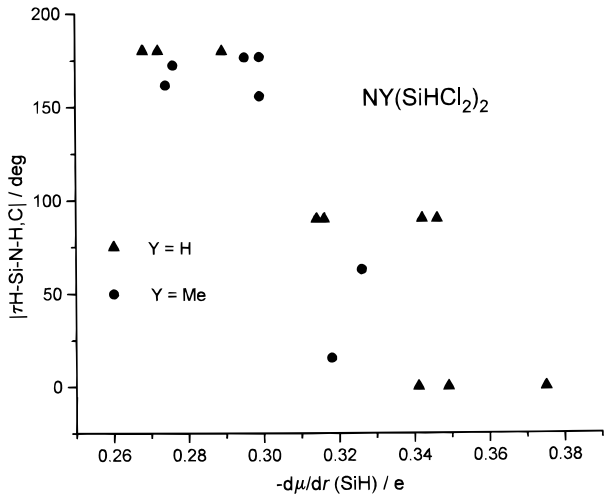

Figure 4. Correlation between $\partial\boldsymbol{\mu}/\partial r$(SiH) and the torsional angle $|\tau H-Si-N-H,C|$ for $NH(SiHCl_2)_2$ and $NMe(SiHCl_2)_2$.

TABLE 12: HF/6-31G* Data for SiCl Bonds in $NH(SiHCl_2)_2$ Structures

	structure					
quantity[a]	**IV**	**V**	**VI**	**VII**	**VIII**	**IX**
rSi_1Cl_{1a}	2.0487	2.0460	2.0441	2.0441	2.0384	2.0451
rSi_1Cl_{1b}	2.0487	2.0483	2.0512	2.0531	2.0507	2.0456
rSi_2Cl_{2a}	2.0487	2.0526	2.0406	2.0439	2.0508	2.0451
rSi_2Cl_{2b}	2.0487	2.0484	2.0507	2.0534	2.0384	2.0456
fSi_1Cl_{1a}	3.3107	3.3352	3.3544	3.3556	3.4162	3.3459
fSi_1Cl_{1b}	3.3107	3.3234	3.2785	3.2701	3.3038	3.3388
fSi_2Cl_{2a}	3.3107	3.2668	3.4007	3.3589	3.3025	3.3459
fSi_2Cl_{2b}	3.3107	3.3128	3.2988	3.2672	3.4171	3.3388
$f'_{1a,1b}$	0.2074	0.1774	0.2066	0.1813	0.1817	0.2084
$f'_{2a,2b}$	0.2074	0.2083	0.1779	0.1813	0.1817	0.2084
$f'_{1a,2a}$	0.0276	0.0110	0.0462	0.0335	0.0137	0.0119
$f'_{1a,2b}$	0.0355	0.0216	0.0208	0.0105	0.0540	0.0512
$f'_{1b,2a}$	0.0355	0.0296	0.0197	0.0105	0.0337	0.0512
$f'_{1b,2b}$	0.0276	0.0312	0.0149	0.0337	0.0137	0.0119
$DCl_{1a}Cl_{2a}$	6.192	5.486	3.909	3.847	5.700	5.160
$DCl_{1a}Cl_{2b}$	5.238	4.914	5.618	5.760	3.719	3.969
$DCl_{1b}Cl_{2a}$	5.238	6.047	4.425	5.760	5.709	3.969
$DCl_{1b}Cl_{2b}$	6.192	5.584	5.843	5.897	5.700	5.164
$\tau Cl_{1a}Si_1NH$	−59.5	−149.1	119.4	−147.0	−147.8	119.6
$\tau Cl_{1b}Si_1NH$	59.5	−28.9	−120.0	−27.7	−27.4	−119.5
$\tau Cl_{2a}Si_2NH$	−59.5	−59.5	−148.8	−146.9	27.4	119.6
$\tau Cl_{2b}Si_2NH$	59.5	58.7	−28.5	−27.6	147.8	−119.5
$\tau Cl_{1a}SiSiCl_{2a}$	−141.8	139.0	−25.3	61.6	−122.8	−110.3
$\tau Cl_{1a}SiSiCl_{2b}$	0.0	−82.5	94.5	177.3	0.0	0.1
$\tau Cl_{1b}SiSiCl_{2a}$	0.0	−104.6	84.4	177.3	0.0	0.1
$\tau Cl_{1b}SiSiCl_{2b}$	141.8	33.8	−155.8	−67.0	122.8	110.5

[a] Si_iCl_i bond lengths $rSiCl_i$ in Å; Si_iCl_i stretching force constants $fSiCl_i$ and stretch−stretch interaction force constants f_{ij}' in aJ $Å^{-2}$; Cl···Cl interatomic distances DCl_iCl_j in Å; torsional angles τCl_iSi_iNY and $\tau Cl_iSiSiCl_j$ in deg.

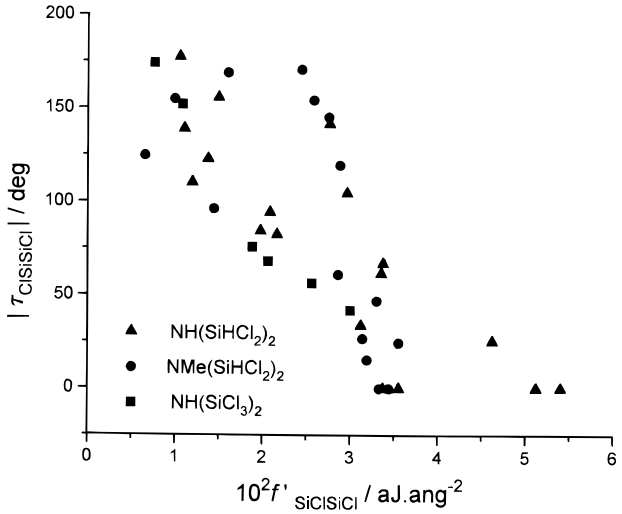

Figure 5. Correlation between $f'_{SiClSiCl}$ and $|\tau$Cl−Si−Si−Cl| for NY-$(SiHCl_2)_2$ (Y = H, Me) and $NH(SiCl_3)_2$.

correlation emerges. The largest value of f', 0.054 aJ Å^{-2}, occurs in structure **VIII**, where DClCl is only 3.719 Å. However, DClCl values for the other pairs of atoms are almost identical, whereas the f' values differ markedly. A similar small value of DClCl in structure **VII** leads to the same f' value as that for DClCl = 5.897 Å. A slightly better correlation is found between f' and τClSiSiCl, the lowest values all being found where $|\tau$ClSiSiCl| is high. This is shown in Figure 5, which includes data for three chlorinated disilazanes. At this stage, all that can be said is that a number of factors must be influencing this interaction between SiCl bonds. This is perhaps not surprising since similar amounts of silicon and chlorine movement will be involved in the stretching of an SiCl bond, unlike the situation with SiH bonds, so that interaction via the SiN bond systems is as likely as "through space" ones between the chlorines.

$\partial\boldsymbol{\mu}/\partial r$ values for the SiCl bond were calculated for all the structures in Table 10. These fell in the range −1.178 to −1.044 e, the vector lying off the bond direction by 2.6−6.4°. For two comparable structures of the $NH(SiHCl_2)_2$ (**IV**) and NMe-$(SiHCl_2)_2$ compounds (**I** in ref 23), $\partial\boldsymbol{\mu}/\partial r$ values were −1.160 and −1.138 e, respectively, showing a modest effect of methyl substitution. There is an overall tendency for $\partial\boldsymbol{\mu}/\partial r$ to increase with τClSiNY, a correlation plot of these two parameters resembling that for the SiH bond in Figure 4.

General Discussion. Several of the properties of the $HNSi_2$ system show interesting effects of substitution. The most striking of these is the variation in the $\delta_\perp$NH bending constant. Table 13 summarizes the information so far available from HF/6-31G* force fields for the two kinds of bending motion.

The most comparable set of numbers are those for the unscaled force field in the second and third columns. The $\delta_\parallel$NH constants decrease slightly as chlorine atoms are replaced by methyl groups, with some variation between the conformers of a given compound. However, the lowering is far more pronounced for the $\delta_\perp$NH constants, for which we quote also the scaled values where these have been determined, to show that the overall trend is virtually independent of the scaling. The chemical interpretation is obvious—the inductive effect of methyl substitution at the Si atom opposes the stabilization of planarity, which is the consequence of nitrogen lone pair donation into the NSi bonds. However, the reverse effect of chlorine appears to be minor, compared with that of hydrogen, judging from the similarity of the constants for the $SiCl_3$ and SiH_3 compounds. To this conclusion we may add the comment

TABLE 13: NH Bending Force Constants (aJ) in Disilazanes

compound, conformer	$F_{unsc}(\parallel)^a$	$F_{unsc}(\perp)^a$	scale factor for ⊥ mode	$F_{sc}(\perp)^b$
$NH(SiCl_3)_2$	0.5055	0.1329	0.6652	0.0884
$NH(SiHCl_2)_2$, **I**	0.4758	0.1172	0.6965	0.0816
$NH(SiHCl_2)_2$, **II**	0.4711	0.0827	0.7036	0.0582
$NH(SiHCl_2)_2$, average	0.4735	0.1000	0.7001	0.0700
$NH(SiMeCl)_2$, *rac A*[c]	0.4798	0.0974	(0.7001)	0.0682
$NH(SiMeCl)_2$, *rac B*[c]	0.4285	0.0690	(0.7001)	0.0483
$NH(SiMeCl)_2$, *rac C*[c]	0.4858	0.0924	(0.7001)	0.0647
$NH(SiMeCl)_2$, *meso A*[c]	0.4565	0.0745	(0.7001)	0.0522
$NH(SiMeCl)_2$, *meso C*[c]	0.5358	0.1058	(0.7001)	0.0741
$NH(SiMeCl)_2$, average	0.4773	0.0878	(0.7001)	0.0615
$NH(SiMe_3)_2$	0.4605	0.0521	(0.6652)	0.0346
$NH(SiMe_3)_2$			(0.7001)	0.0364
$NH(SiH_3)_2$[d]	0.4597	0.1242	(0.7001)	0.0870

[a] From the unscaled HF/6-31G* force field. The coordinate for the $\delta_\parallel$NH mode is $2^{-1/2}(\delta HNSi_1 - \delta HNSi_2)$. For the $\delta_\perp$NH one, we use that recommended by Hedberg and Mills which is applicable to both planar and nonplanar four-atom systems.[27] Units: aJ. [b] After scaling to observed frequencies, except for constrained values in parentheses. [c] From the force fields determined in ref 13. [d] Current work in our laboratories. The $HNSi_2$ skeleton in this molecule is calculated to be nonplanar by 3.1° at the HF/6-31G* level. An analogous calculation for $N(SiH_3)_3$ gives an almost identical value for $F_{unsc}(\perp)$ (0.1292 aJ), accompanied by an out-of-plane bending frequency of 206 cm^{-1}. The actual frequency will be substantially less than this, in contrast to earlier estimates of 312[33] and 434 cm^{-1}.[34]

TABLE 14: Properties of the NH Bond in Disilazanes

compound conformer	νNH_{unsc}/cm^{-1} [a]	$A(\nu NH)$/km mol^{-1} [b]	q_H/e[c]
$NH(SiCl_3)_2$	3746	89.0	0.430
$NH(SiHCl_2)_2$, **I**	3741	71.5	0.424
$NH(SiHCl_2)_2$, **II**	3749	75.5	0.421
$NH(SiHCl_2)_2$, average	3745	73.5	0.423
$NH(SiMeCl)_2$, *rac A*[d]	3750	41.8	0.400
$NH(SiMeCl)_2$, *rac B*[d]	3760	37.8	0.395
$NH(SiMeCl)_2$, *rac C*[d]	3764	55.5	0.404
$NH(SiMeCl)_2$, *meso A*[d]	3761	45.2	0.400
$NH(SiMeCl)_2$, *meso C*[d]	3747	50.0	0.403
$NH(SiMeCl)_2$, average	3751	46.1	0.400
$NH(SiMe_3)_2$	3771	18.7	0.369
$NH(SiH_3)_2$[e]	3773	32.9	0.382

[a] Unscaled frequency from the HF/6-31G* force field. [b] Infrared intensity. [c] Mulliken charge on the hydrogen atom. [d] Data accompanying the calculations in ref 13. [e] Current work in our laboratories.

that since the HF scale factor for $\delta_\perp$NH bending is markedly lower than is normal for bending motions, the stability of the planar arrangement is significantly overestimated at this level of computation in all the compounds.

In Table 14 we display some data for the NH bond, including the unscaled stretching frequency, its infrared intensity, and the Mulliken charge on the hydrogen atom. (We avoid quoting the scaled frequencies since these are based on both gas- and liquid-phase data, the latter of which carry uncertain shifts due to condensation.)

There is some variation among the conformers of a given molecule, especially for the SiHMeCl compound, but when averages are taken, the interchange of methyl and chlorine has no significant effect on νNH. However, there is a marked one on infrared intensity. By comparison with $NH(SiH_3)_2$, chlorine enhances and the methyl group reduces intensity. To a minor extent, this reflects variations in the Mulliken charge on the hydrogen atom which becomes slightly less positive with the substitution of methyl, slightly more so as chlorine is added, but the major effect on the dipole derivative $\partial\boldsymbol{\mu}/\partial r$ would appear to be through a charge flux term.[32]

Acknowledgment. We are greatly indebted to Dr. M. Bühl for extending his earlier calculations on $NH(SiHCl_2)_2$, to Professor H. Bürger for the νSiH spectra fitted in Figure 2, and to a reviewer for a careful reading of the paper and helpful comments. We also thank Drs. B. A. Smart and C. Morrison for patient tuition in the use of the program Gaussian 94, the EPSRC for the Edinburgh ab initio facility funded by grant GR/K/04194, and the Fonds der chemischen Industrie for a research grant (H.F.).

References and Notes

(1) Hedberg, K *J. Am. Chem. Soc.* **1955**, *77*, 6491.
(2) Beagley, B.; Conrad, A. R. *Trans. Faraday Soc.* **1970**, *66*, 2740.
(3) Rankin, D. W. H.; Robiette, A. G.; Sheldrick, G. M.; Sheldrick, W. S.; Aylett, B. J.; Ellis, I. A.; Monaghan, J. J. *J. Chem. Soc. A* **1969**, 1224.
(4) Glidewell, C.; Rankin, D. W. H.; Robiette, A. G.; Sheldrick, G. M. *J. Mol. Struct.* **1969**, *4*, 215.
(5) Anderson, D. G.; Rankin, D. W. H. *J. Mol. Struct.* **1989**, *195*, 261.
(6) Fjeldberg, T. *J. Mol. Struct.* **1984**, *112*, 159.
(7) Gunderson, G.; Rankin, D. W. H. *Acta Chem. Scand.* **1984**, *A38*, 647.
(8) Gunderson, G.; Rankin D. W. H.; Robertson, H. E. *J. Chem. Soc., Dalton Trans.* **1985**, 191.
(9) Rankin, D. W. H.; Robertson, H. E. *J. Chem. Soc., Dalton Trans.* **1987**, 785.
(10) Anderson, D. G.; Rankin, D. W. H. *J. Chem. Soc., Dalton Trans.* **1989**, 779.
(11) Fleischer, H.; Hnyk, D.; Rankin, D. W. H.; Robertson, H. E.; Bühl, M.; Thiel, W. *Chem. Ber.* **1995**, *128*, 807.
(12) Fleischer, H.;. Brain, P. T.; Rankin, D. W. H.; Robertson, H. E.; Bühl, M.; Thiel, W. *J. Chem. Soc., Dalton Trans.* **1998**, 593.
(13) Fleischer, H.; McKean, D. C.; Pulham, C. R.; Bühl, M. *J. Chem. Soc., Dalton Trans.* **1998**, 585.
(14) McKean, D. C.; Torto, I. *Spectrochim. Acta* **1993**, *49A*, 1095.
(15) Bürger, H.; Burczyk, K.; Höfler, F.; Sawodny, W. *Spectrochim. Acta* **1969**, *25A*, 1891.
(16) Cerato, C. C.; Lauer, J. L.; Beachell, H. C. *J. Chem. Phys.* **1954**, *22*, 1.
(17) Kriegsmann, H. *Z. Elektrochem.* **1957**, *8*, 1088.
(18) Goubeau, J.; Jimenz-Barbera, J. *Z. Anorg. Allg. Chem.* **1960**, *303*, 15.
(19) Marchand, A.; Forel, M.-T.; Metras, F.; Valade, J. *J. Chim. Phys.* **1964**, 344.
(20) Hamada, K.; Morishita, H. *Spectrosc. Lett.* **1983**, *16*, 717.
(21) Fleischer, H.; Hensen, K.; Burgdorf, D.; Flindt, R.; Wannagat, U.; Bürger, H.; Pawelke, G. *Z. Anorg. Allg. Chem.* **1995**, *621*, 239.
(22) McKean, D. C.; Edwards, H. G. M.; Lewis, I. R.; Murphy, W. F.; Mastryukov, V. S.; Boggs, J. E. *Spectrochim. Acta* **1995**, *51A*, 2237.
(23) McKean, D. C. *Spectrochim. Acta*, in press.
(24) Fleischer, H.; McKean, D. C.; Parsons, S.; Bühl, M. *Z. Anorg. Allg. Chem.*, in press.
(25) Frisch, M. J.; Trucks, G. W.; Schlegel, H. B.; Gill, P. M. W.; Johnson, B. G.; Robb, M. A.; Cheeseman, J. R.; Keith, T. A.; Petersson, G. A.; Montgomery, J. A.; Raghavachari, K.; Al-Laham, M. A.; Zakrzewski, V. G.; Ortiz, J. V.; Foresman, J. B.; Cioslowski, C.; Stefanov, B. B.; Nanayakkara, A.; Challacombe, M.; Peng, C. Y.; Ayala, P. Y.; Chen, W.; Wong, M. W. ; Andres, J. L.; Replogle, E. S.; Gomperts, R.; Martin, R. L.; Fox, D. J.; Binkley, J. S.; Defrees, D. J.; Baker, J.; Stewart, J. P.; Head-Gordon, M.; Gonzalez, C.; Pople, J. A. *Gaussian 94*, Revision C2; Gaussian Inc.: Pittsburgh, PA, 1995.
(26) Hehre, W. J.: Radom, L.; Schleyer, P. v. R.; Pople, J. A. *Ab initio Molecular Orbital Theory*; Wiley: New York, 1986.
(27) Hedberg, L.; Mills, I. M. *J. Mol. Spectrosc.* **1993**, *160*, 117.
(28) Pulay, P.; Fogarasi, G.; Pang, F.; Boggs, J. E. *J. Am. Chem. Soc.* **1979**, *101*, 2550.
(29) Person, W. B.; Newton, J. H. *J. Chem. Phys.* **1974**, *61*, 1040.
(30) King, W. T.; Mast, G. B.; Blanchette, P. P. *J. Chem. Phys.* **1972**, *56*, 4440.
(31) Murphy, W. F.; Zerbetto, F.; Duncan, J. L.; McKean, D. C. *J. Phys. Chem.* **1993**, *97*, 581.
(32) Gussoni, M.; Jona, P.; Zerbi, G. *J. Chem. Phys.* **1983**, *78*, 6802.
(33) Miller, F. A.; Perkins, J.; Gibbon, G. A.; Swisshelm, B. A. *J. Raman Spectrosc.* **1974**, *2*, 93.
(34) Goldfarb, T. D.; Khare, B. N. *J. Chem. Phys.* **1967**, *46*, 3379.